ADVANCED FUNCTIONAL MATERIALS

DOI: 10.1002/adfm.200700067

Sandwiched Ruthenium/Carbon Nanostructures for Highly Active Heterogeneous Hydrogenation**

By *Fabing Su, Fang Yin Lee, Lu Lv, Jiajia Liu, Xiao Ning Tian,* and *Xiu Song Zhao**

The immobilization of metal nanoparticles in the framework of porous carbon for heterogeneous catalysis may avoid particle aggregation, movement, and leaching, thus leading to a high catalyst efficiency. In this Full Paper, an approach to prepare Ru nanoparticles incorporated into the pore walls of porous carbon to form a sandwiched Ru/C nanostructure for heterogeneous hydrogenation is demonstrated. Physical adsorption of nitrogen, X-ray diffraction, thermogravimetric analysis, field-emission transmission electron microscopy, field-emission scanning electron microscopy, and energy dispersive X-ray spectroscopy techniques are employed to study the structure and morphology of the catalysts. Catalytic results show that the Ru nanoparticles sandwiched in the pore walls of porous carbon display a remarkably high activity and stability in the hydrogenation of benzene. An enhanced hydrogen spillover effect is believed to play a significant role in the hydrogenation reaction because of the intimate interfacial contact between Ru nanoparticles and the carbon support. The catalyst system described in this work may offer a new concept for optimizing catalyst nanostructures.

1. Introduction

Since the discovery of ruthenium as a catalyst for hydrogenation reactions,[1] Ru catalysts have been widely used in the chemical, petrochemical, food, and pharmaceutical industries, and in energy-conversion technologies. The scope of homogeneous Ru catalysts has been well-illustrated recently.[2] However, heterogeneous catalysts can be preferable from both industrial and environmental perspectives.

Recently, Miao et al.[3] described a method for preparing Ru catalysts by immobilizing Ru nanoparticles on montmorillonite (MMT) clay with the assistance of ionic liquids. While the Ru/MMT catalyst exhibited excellent activity for the hydrogenation of benzene, the Ru nanoparticles were found to aggregate to form larger particles after several reaction runs. Sun et al.[4] reported immobilization of Ru colloidal particles on carbon nanotubes via supercritical water. However, the use of carbon nanotubes as a catalyst support can be quite limited because of their low specific surface area. It should be mentioned that in both papers,[3,4] the authors observed that the immobilized Ru catalysts tended to be easily oxidized upon exposure to air, thus, resulting in loss in catalytic activity. Additionally, Ru nanoparticles highly dispersed on the pore surfaces of mesoporous silicas,[5] supported on alkali-exchanged zeolite Beta,[6] on the surfaces of activated carbons,[7] alumina, and titanium oxides[8] prepared by using conventional methods were reported as well. However, these methods suffer from a number of problems, such as particle aggregation and catalyst leaching. Thus, searching for an alternative approach to preparing Ru catalysts with high stability and catalytic activity is receiving rapidly growing attention.

The hard-template strategy for synthesizing templated porous carbon (TPC) materials[9] has opened up opportunities for exploring novel heterogeneous catalysts.[10] Lu et al.[10c] fabricated a Pd/Co–TPC catalyst with Co nanoparticles immobilized on the external surface of TPC to facilitate magnetic recovery in a reaction system. Chai et al.[10d] described a Pt–TPC electrocatalyst with Pt nanoparticles embedded in the carbon wall of TPC, which displayed good electrochemical catalytic performance. The encapsulation of Fe, Co, and Ni metal nanoparticles in TPCs as magnetically separable adsorbents was reported.[11] It is to be noted that such metal particles embedded in TPCs are extremely stable against leaching[11] while the pores of the carbon are highly accessible.[10d] More interestingly, the template method also offers chances for developing novel catalyst systems, which are rarely obtained with traditional preparation methods. For example, Lee et al.[12] demonstrated the fabrication of a magnetically switchable bio-electrocatalytic system with immobilized enzymes for the oxidation of glucose based on templated mesocellular carbon. Ikeda et al.[13] described novel Pt–TPC catalyst systems with Pt nanoparticles encapsulated in a hollow porous carbon shell as a highly active heterogeneous hydrogenation catalyst. The development of these novel heterogeneous catalyst systems is very

[*] Prof. X. S. Zhao, Dr. F. Su, Dr. L. Lv, J. Liu, X. N. Tian
Department of Chemical and Biomolecular Engineering
National University of Singapore
4 Engineering Drive 4, Singapore 117576 (Singapore)
E-mail: chezxs@nus.edu.sg
Prof. X. S. Zhao, F. Y. Lee
Nanoscience and Nanotechnology Initiative
National University of Singapore
2 Science Drive 3, Singapore 11754 (Singapore)

[**] This work was supported by the National University of Singapore (NUS). Supporting Information is available online from Wiley InterScience or from the author.

ADVANCED FUNCTIONAL MATERIALS

helpful for optimizing catalyst nanostructures and understanding catalytic mechanisms.

In the present Full Paper, we demonstrate the fabrication of a new nanostructured catalyst system with Ru nanoparticles sandwiched in the pore walls of TPCs. The preparation procedure is schematically illustrated in Scheme 1. First, Ru nanoparticles were impregnated on the pore surface of a hard template (either zeolite HY or mesoporous silica, SBA-15). Second, infiltration of carbon in the pores of the template was conducted using the chemical vapor deposition (CVD) method with benzene as a carbon precursor.[14] Finally, the template was removed using a HF solution to yield porous carbon with Ru nanoparticles sandwiched in the carbon matrix.

The Ru nanocatalysts thus obtained with HY and SBA-15 as templates are designated as RuC1 and RuC2, respectively. A number of advantages of such Ru/C nanostructured catalysts over those prepared using conventional methods can be anticipated, such as firm fixation of the Ru nanoparticles in the carbon matrix, no aggregation of the Ru nanoparticles, no pore blocking, an extremely intimate contact between the metal and support, controllable Ru nanoparticle size, and tailorable pore size of the support. To evaluate the catalytic properties of catalysts RuC1 and RuC2, we employed benzene hydrogenation because it is a model reaction of catalytic transformation of aromatics[15] and also of significance in the production of high-quality fuels.[16] Both RuC1 and RuC2 catalysts displayed excellent catalytic activity, high stability, and negligible leaching.

2. Results and Discussion

Figure 1 shows the field-emission scanning electron microscopy (FESEM) images of the templates and catalysts. It can be seen that both catalysts display a similar morphology to their respective hard-template counterparts, indicating they were replicated from the hard templates. It is also seen that the particle size of catalyst RuC1 is smaller than that of catalyst RuC2.

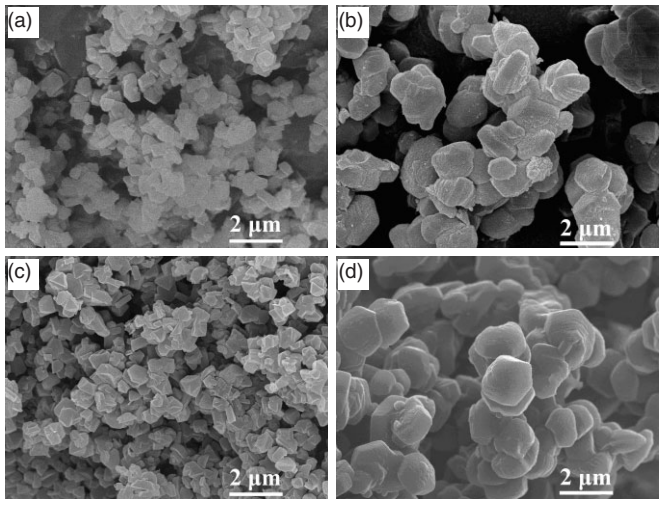

Figure 1. FESEM images of the hard templates: zeolite HY (a) and SBA-15 (b), and the respective catalysts: RuC1 (c) and RuC2 (d).

Figure 2a shows the transmission electron microscopy (TEM) image of catalyst RuC1. It is seen that the Ru nanoparticles, imaged as dark dots on the gray carbon background, are uniformly dispersed within the carbon framework, except for one larger black spot, which was probably formed on the external surface of zeolite HY. The Ru particle sizes range from 1 to 2 nm, comparable to that of the channel and cage sizes of zeolite Y, showing that the Ru particles were confined in the pores of HY and incorporated in the carbon matrix. Using SBA-15 silica as template, Ru nanoparticles of 7–8 nm in diameter were obtained, as can be seen from Figure 2b, agreeing well with the pore-channel size of SBA-15 (7–8 nm). It is also clearly seen that the Ru particles were obviously sandwiched in the arrayed pore walls of the mesoporous carbon. Such a Ru/C nanostructure can thus effectively prevent Ru nanoparticles from both aggregation and leaching while remaining accessible. It is also seen that the mesoporous channels are not blocked by the Ru nanoparticles, thus greatly facilitating the transport of both reactant and product. The TEM images with a lower magnification (see Supporting Information, Fig. S1) further confirmed the presence of Ru nanoparticles incorporated in the carbon framework. An analysis of energy-dispersive X-ray (EDX) spectra showed that the Ru content was about 8.0 wt % in RuC1 and 9.8 wt % in RuC2; values that are consistent with thermal gravimetric analysis (TGA) data (see Fig. S2), which showed the Ru content in catalysts RuC1 and RuC2 to be about 7.8 and 9.3 wt %, respectively.

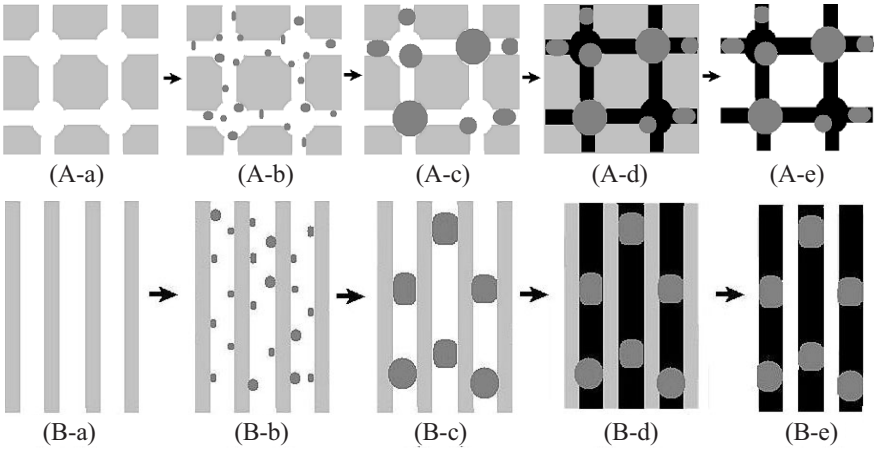

Scheme 1. A schematic illustration of the preparation procedure using zeolite HY (A) and mesoporous silica SBA-15 (B) as templates: a) hard template; b) RuO_2 nanoparticles confined in the pores of the template by the impregnation method; c) RuO_2 nanoparticles grow at high temperature in nitrogen gas; d) infiltration of carbon into the pores using the CVD method; e) Ru nanoparticles sandwiched in the carbon matrix upon removal of the template.

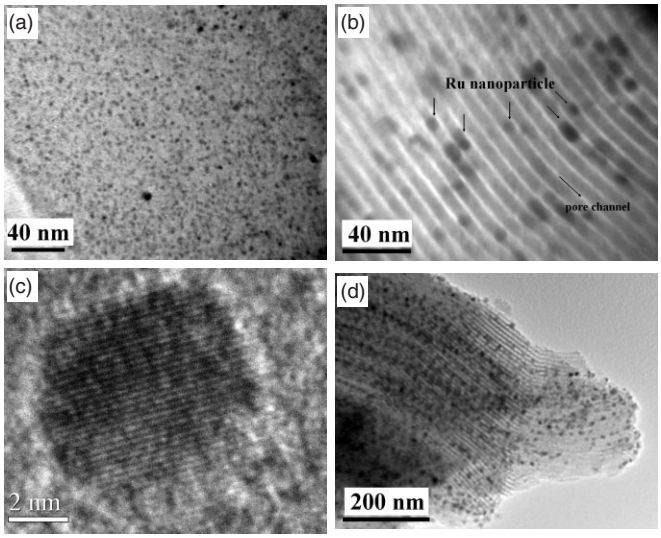

Figure 2. TEM images of catalysts RuC1 (a) and RuC2 (b), a single Ru nanocrystal taken from RuC2 (c), and a sample of RuO_2/SBA-15 (d).

Figure 2c shows the TEM image of a single Ru nanocrystal with a diameter of around 7 nm taken from catalyst RuC2. Aligned crystal lattices with an average spacing of about 0.21 nm, corresponding to the (101) plane of Ru,[17] are seen. Figure 2d shows the TEM image of RuO_2/SBA-15, a sample collected at Step B-c in Scheme 1. Many black dots, representing RuO_2 particles as confirmed by X-ray diffraction (XRD), are arrayed in the highly ordered pore channels of SBA-15. These particles were formed from smaller ones because of particle aggregation during the high-temperature treatment step, and subsequently reduced to metallic Ru nanoparticles by carbon species and/or insufficient hydrogen during the CVD process (see the discussion below).

Compared in Figure 3 are the XRD patterns of catalysts RuC1, RuC2, and sample RuO_2/SBA-15. The peaks at 28.1°, 35.1°, 44.0°, 54.4°, and 57.7° observed on sample RuO_2/SBA-15 can be indexed to the (110), (101), (111), (211), and (220) planes, respectively, of anhydrous crystalline RuO_2 (International Center for Diffraction Data of the Joint Committee on Powder Diffraction Standards (JCPDS-ICDD) card No. 43-1027) with a rutile-type structure. The peaks at 38.3°, 42.2°, 44.0°, 58.3°, 69.5°, and 78.4° seen on catalysts RuC1 and RuC2 can be respectively assigned to (100), (002), (101), (102), (110), and (103) diffraction planes of bulk hexagonal Ru metal (JCPDS-ICDD card No. 06-0663). The relatively sharp peaks may be due to the few large Ru particles formed on the external surface of the template. No diffraction peak at around 35° can be seen on the two catalysts, suggesting a complete reduction of RuO_2 to Ru by carbon species and/or insufficient hydrogen gas released from benzene dehydrogenation during the CVD process.[18] In contrast, no peaks associated with Ru metal are seen in the XRD patterns of Ru/C1 and Ru/C2, shown in Figure S3a of the Supporting Information, probably due to the too small Ru particle size (see Fig. S3b and c). These two catalysts were prepared using the conventional impregnation method followed by hydrogen reduction with template microporous carbon C1 and template mesoporous carbon C2 as the supports, which were prepared as described previously.[14] Here, it should be noted that the hydrogen reduction for Ru/C1 and Ru/C2 could not be carried out at 900 °C due to the methanation or gasification of carbon at high temperatures catalyzed by Ru.[19]

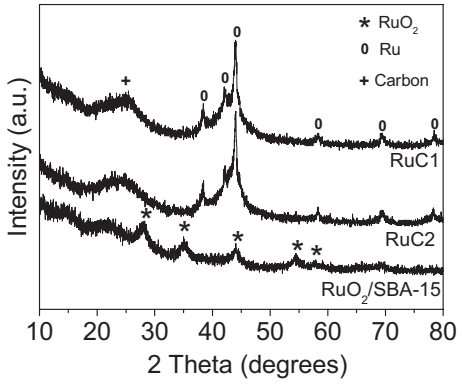

Figure 3. XRD patterns of RuC1, RuC2, and RuO_2/SBA-15.

The N_2 adsorption–desorption isotherms and pore size distribution (PSD) curves of catalysts RuC1 and RuC2 are shown in Figure 4, and the pore structure parameters are compiled in Table 1. According to the IUPAC classification, the adsorption

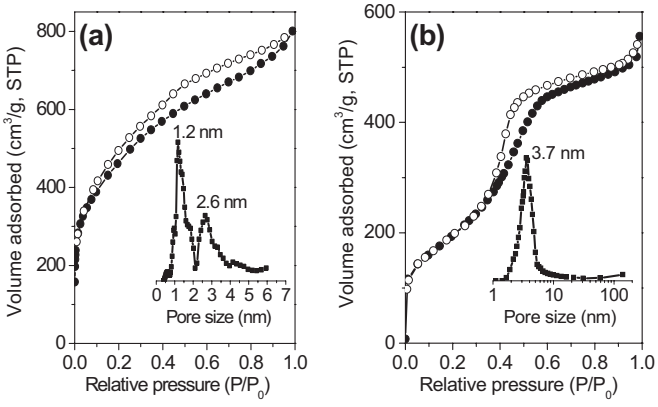

Figure 4. Nitrogen adsorption–desorption isotherms (STP: standard temperature and pressure) and respective PSD curves (inset) of RuC1 (a) and RuC2 (b) (full circles: adsorption branch, empty circles: desorption branch).

Table 1. Physicochemical properties of Ru catalysts.

Sample	S_{BET} [a] [m^2 g^{-1}]	V_t [b] [cm^3 g^{-1}]	D [c] [nm]	C_{Ru} [d] [ppb]
RuC1	1690	1.23	1.2	16
RuC2	708	0.83	3.7	10
Ru/C1	1504	1.10	1.2	73
Ru/C2	650	0.80	3.8	1027
Ru/HY1	695	0.33	1.2	37
Ru/SBA-15	614	0.77	7.9	515
Ru/HY2	503	0.20	1.1	–

[a] Brunauer–Emmett–Teller surface area. [b] Total pore volume. [c] Pore diameter. [d] Ru concentration in solution after 2 h ultrasonication.

ADVANCED FUNCTIONAL MATERIALS

isotherm of RuC1 is of type I, indicating the dominance of micropores. The type IV isotherm together with a H2 hysteresis loop of catalyst RuC2 indicates it is a mesoporous material. The specific surface areas were calculated to be 1690 and 708 $m^2 g^{-1}$ and the pore volumes were estimated to be about 1.23 and 0.83 $cm^3 g^{-1}$, respectively, for catalysts RuC1 and RuC2. The main pore size of catalyst RuC1, calculated using the density functional theory (DFT) method, was around 1.2 nm while that of RuC2, calculated using the Barrett–Joyner–Halenda (BJH) method, was centered at 3.7 nm. Also included in Table 1 are the physicochemical properties of other Ru catalysts for comparison purposes, suggesting that the surface area, pore volume, and pore size of RuC1 and RuC2 are comparable to those of Ru/C1 and Ru/C2, respectively.

Table 2 shows the catalytic properties of the Ru catalysts prepared in this work in hydrogenation of benzene under various conditions. Both RuC1 and RuC2 catalysts showed a remarkably higher catalytic activity (entries 1–7) than the Ru catalysts prepared using the hydrogen reduction method (entries 8–12) and Ru/MMT,[3] which was reported to out-perform several commercial catalysts. The activities of RuC1 (entry 2) and RuC2 (entry 4) are around five times of that of Ru/C1 (entry 8) and Ru/C2 (entry 9), and much higher than that of catalysts Ru/HY1 (entry 10), Ru/SBA-15 (entry 11), and Ru/HY1 (entry 12), which were prepared under different conditions. In addition, although the 86.5 % conversion of benzene on catalyst RuC1 (entry 1) is comparable to that on catalyst Ru/MMT (84.5 %) reported in the literature,[3] the molar ratio of benzene/Ru used in this work was 4000, higher than the literature value of 1000.[3] Remarkably, the activity of catalyst RuC2 at 110 °C and 8 MPa was measured to be some 10 000 (entry 6), about 2.5 times higher than that of catalyst Ru/MMT (4000).[3] The catalytic activity of catalysts RuC1 and RuC2 is also much higher than that of a hybrid catalyst Rh^{I}-Pd^{0}/SiO_2.[20]

After the first run of catalytic reaction, catalysts RuC1 and RuC2 were recycled, dried at 120 °C in air, and reused without hydrogen reduction. Surprisingly, loss in catalytic activity was not observed even after three or five reaction runs (entries 5 and 3, respectively). In addition, long-term storage (1 year) under ambient conditions did not lead to obvious deterioration in catalytic performance (entry 7). Neither aggregation of Ru nanoparticles (see Fig. S1b and c) nor loss in Ru content (see Fig. S2) after five reaction runs was observed. Furthermore, the much lower Ru concentrations of RuC1 and RuC2 in water after 2 h ultrasonication (see Table 1) demonstrate their negligible leaching compared with other catalysts. Therefore, the Ru catalysts prepared in this work are highly stable and reusable.

It has been seen that the Ru nanoparticle size of RuC1 and RuC2 is distinctly larger than that of Ru/C1 and Ru/C2 (see Fig. 2 and Fig. S3), but the catalytic activity of the former pair of catalysts is definitely better than that of the latter, although we could exclude the effect of pore structure. On the other hand, RuC1 and RuC2 possess an obvious difference in catalyst particle size (see Fig. 1), Ru nanoparticle size (see Fig. 2), and pore structure (see Fig. 4 and Table 1), but their catalytic activities are comparable. Therefore, factors other than particle size and pore structure must account for the high catalytic activity. The sandwiched Ru/C nanostructure may be responsible for the observed high catalytic activity and stability. It is well known that hydrogen spillover always exerts a great influence on the catalytic activity, selectivity, and stability of many heterogeneous catalysts in hydrogenation reactions.[21,22] The spillover of the dissociated hydrogen species of a metal onto its support surface is highly dependent upon the metal/support interface because the process involves mass transfer of electrons and hydrogen spillover species (H_{so}).[23–25] It has been known that hydrogen could be adsorbed dissociatively on the exposed Ru surface to form atomic H_{so} immediately followed by spillover onto the various supports.[26] In the present case, the sandwiched Ru catalysts created an highly intimate contact between the Ru nanoparticle and the carbon support because of the carbon deposition on the Ru surface via CVD; thus, forming a close surface contact as suggested by the results shown in Figure S4. Such intimate contact, greatly enhanced the transfer rate of H_{so} species, which then hydrogenated benzene, adsorbed on the pore surface of the support,[27] to form cyclohexane, resulting in the observed high catalytic activity. Other factors, such as the unblocked nanopores, absence of chloride species[28] (X-ray photoelectron spectroscopy analysis, not shown here) because of the high-temperature conditions, the electronic effect of the Ru particle as well as its special circumstance being surrounded by carbon (reducing agent), may also account for the excellent catalytic performance to some extent.

It is noteworthy that, although our results unambiguously prove that the sur-

Table 2. Hydrogenation activities of various supported Ru catalysts (*T*: temperature; *P*: pressure; *t*: time).

Entry	Ru catalyst	Ru [wt %]	Benzene/Ru [a]	*T* [°C]	*P* [H_2, MPa]	*t* [h]	Conversion [%] [b]	Activity [h^{-1}] [c]
1	RuC1	7.8	4000:1	40	2.0	2.5	86.5	1384
2	RuC1	7.8	10000:1	110	4.0	1.9	99.6	5242
3	RuC1 (5th) [d]	7.8	10000:1	110	4.0	1.9	99.5	5237
4	RuC2	9.3	10000:1	110	4.0	1.8	99.8	5544
5	RuC2 (3rd) [e]	9.3	10000:1	110	4.0	1.8	99.7	5539
6	RuC2	9.3	10000:1	110	8.0	1.0	99.8	9980
7	RuC2 (1y) [f]	9.3	10000:1	110	4.0	1.8	99.5	5528
8	Ru/C1	8.7	10000:1	110	4.0	2.0	21.5	1075
9	Ru/C2	7.1	10000:1	110	4.0	2.0	20.0	1000
10	Ru/HY1	6.2	10000:1	110	4.0	2.0	15.3	765
11	Ru/SBA-15	6.6	10000:1	110	4.0	2.0	24.0	1200
12	Ru/HY2 [g]	3.3	10000:1	110	4.0	2.0	1.0	/

[a] Molar ratio of benzene over Ru. [b] Conversion of benzene. [c] The activity was calculated as the conversion of moles of benzene per mole of Ru per hour. [d] RuC1 was reused five times. [e] RuC2 was reused three times. [f] RuC2 was used after storage in a plastic bottle for one year. [g] The catalyst was prepared by hydrogen reduction at 900 °C for 2 h.

prising catalytic activity and stability of RuC1 and RuC2 catalysts come from the sandwiched Ru/C nanostructure, the template method used here may make a synthetic approach impractical for industrial applications but could deepen our understanding of the remarkable catalytic properties of carbon-supported Ru catalysts and of the significant role of the metal–carbon contact in benzene hydrogenation. Additionally, we also found enhanced catalytic activity for methanol electro-oxidation when RuC1 and RuC2 were used as Pt-catalyst supports for preparing Pt–Ru bimetallic electrocatalysts. The role of such nanostructures in other reactions or applications, such as ammonium synthesis,[29] selective hydrogenation,[30] hydrogen storage facilitated by hydrogen spillover,[31] and supercapacitors,[32] after Ru oxidation are being explored. The further investigation of hydrogen spillover enhanced by such sandwiched Ru/C nanostructures is really needed and will be helpful for us to design new and industrially practical heterogeneous Ru catalysts.

3. Conclusions

We have demonstrated the preparation of novel Ru/C nanostructured catalysts with Ru nanoparticles incorporated in the pore walls of templated porous carbons by using H-form zeolite (HY) and ordered mesoporous silica (SBA-15) as templates. The Ru nanoparticles thus prepared displayed remarkably high activity and stability in the hydrogenation of benzene because of the hydrogen-spillover effect enhanced by the intimate surface contact between the Ru nanoparticles and the carbon supports, together with the unblocked pores of the catalysts and the firm immobilization and high dispersion of the Ru nanoparticles in the carbon matrix. The present synthesis strategy and concept of metal/carbon nanostructures may allow one to design novel multifunctional catalytic nanoarchitectures.

4. Experimental

Preparation of RuC1 and RuC2 Catalysts: As schematically illustrated in Scheme 1, first, a porous hard template (either H-form zeolite Y, HY, from Zeolyst International Company, or mesoporous SBA-15 silica synthesized according to Zhao et al. [33]) was impregnated with a ruthenium chloride solution ($RuCl_3 \cdot H_2O$, Aldrich) by sonication for 0.5 h. The concentration of the $RuCl_3$ solution used here was 0.1 M and the ratio of solution volume to hard-template mass was 4 mL:1 g. Second, the suspension was evaporated under stirring at 100 °C, and then dried in air at 200 °C for 3 h. Third, the Ru-impregnated solid (around 0.5 g) was placed in a quartz tube and heated to 900 °C under a pure N_2 flow (30 $cm^3 min^{-1}$). Subsequently, infiltration of carbon was conducted with benzene as the carbon precursor using the CVD method at 900 °C for 3 h [14]. Finally, the black sample was treated with a 20 % HF solution to remove the template, washed with deionized water, and dried at 12 °C overnight. The Ru catalysts thus obtained using HY and SBA-15 as hard templates were designated as RuC1 and RuC2, respectively.

Preparation of Other Ru Catalysts Involved in this Study: Two porous carbon supports, designated as C1 and C2, were prepared using HY and pure-silica SBA-15 as templates, respectively, as described previously [14]. C1 and C2 were impregnated with a $RuCl_3$ solution, evaporated, and dried at 120 °C for 3 h, followed by hydrogen reduction at 300 °C for 2 h [28,34] to obtain two supported Ru catalysts, designated as Ru/C1 and Ru/C2, respectively. The preparation of catalysts Ru/HY1 and Ru/SBA-15 was conducted in a similar way as for catalysts Ru/C1 and Ru/C2 except that HY and SBA-15 were used as the supports and drying took place at 200 °C for 3 h. Another catalyst, Ru/HY2, was prepared similarly to Ru/HY1, but with a higher hydrogen-reduction temperature, namely, 900 °C instead of 300 °C. The mass contents of Ru in the catalysts were evaluated based on the amount of the supported Ru catalyst and $RuCl_3$ added [3,28].

Characterization of Samples: The porous properties of the samples were characterized using N_2 adsorption at –196 °C on an automatic volumetric sorption analyzer (Quantachrome, NOVA1200). Prior to adsorption, the samples were degassed at 200 °C for 5 h under vacuum. The Brunauer–Emmett–Teller (BET) method was used to determine the specific surface area of the samples in the relative pressure range (P/P_0) of 0.05–0.2. The total pore volume was obtained from the volume of N_2 adsorbed at the relative pressure of 0.99. The pore size distribution (PSD) curves of the microporous catalysts (RuC1, Ru/C1, Ru/HY1, and Ru-HY2) were calculated using the density functional theory (DFT) method, while PSD curves of the mesoporous samples (RuC2, Ru/C2, and Ru/SBA-15) were derived from the Barrett–Joyner–Halenda (BJH) method using the adsorption branches. The X-ray diffraction (XRD) patterns were collected on an XRD-6000 (Shimadzu, Japan) with Cu Kα radiation. Thermal gravimetric analysis (TGA) was carried out on a thermogravimetric analyzer (TGA 2050, Thermal Analysis Instruments, USA) with an air flow rate of 100 mL min^{-1} and a temperature ramp of 10 °C min^{-1}. The microscopic features of the samples were observed by using a transmission electron microscope (JEM 2010F, JEOL, Japan) operated at 200 kV and a field-emission scanning electron microscope (JSM-6700F, JEOL Japan) operated at 10 kV. EDX spectroscopy was conducted for sample-composition analysis on the TEM instrument. The leaching experiment was carried out as follows: around 100 mg of catalyst placed in 15 mL of water was ultrasonicated for 2 h, and after filtration of the suspension solution, the Ru concentration was determined using an inductively coupled plasma atomic mass spectrometer (Perkin–Elmer ELAN6100) with 100.906 nm as the wavelength of Ru.

Catalytic-Activity Measurements: The evaluation of the catalytic properties of the Ru catalysts for hydrogenation of benzene to cyclohexane was conducted using a 300 mL stainless-steel stirred pressure reactor (Parr Instruments). An appropriate amount of Ru catalyst and 30 mL of benzene (99.9 %, Aldrich) were placed in the reactor. Subsequently, the reactor was purged with highly pure H_2 (> 99.9995 %, Singapore Oxygen Air Liquide Pte. Ltd.) for 5 min. Then, the reaction pressure was generated using H_2 at the reaction temperature. The reactor was stirred at 200 rpm and the pressure was maintained constant using H_2. After a given period of reaction time or after no hydrogen uptake was observed, the reactor was cooled down to room temperature in an ice–water bath and the pressure in the reactor was released. The reactant and products were analyzed using an isocratic high-performance liquid chromatograph (Agilent 1100 series HPLC) system with an Agilent 1100 standard variable wavelength UV detector and an AD-H normal phase column (250 mm × 4.6 mm, 5 μm packing size, Daicel Chemical Industries). The concentration of benzene was quantitatively determined based on the standard calibration curve obtained prior to every analysis using an eluent of 95 % *n*-hexane/5 % isopropyl alcohol at a flow rate of 1 mL min^{-1} under isobaric conditions. Benzene was analyzed at a wavelength of 254 nm, whereas cyclohexane has a UV cut-off at 200 nm. For the comparison, the catalytic activity of a catalyst was calculated as the conversion of moles of benzene per mole of Ru per hour, which is the same as the calculation of the turnover frequency used in a previous report [3].

Received: January 16, 2007
Revised: February 26, 2007
Published online: June 29, 2007

[1] a) J. E. Carnahan, T. A. Ford, W. F. Gresham, W. E. Grigsby, G. F. Hager, *J. Am. Chem. Soc.* **1955**, *77*, 3766. b) L. M. Berkowitz, P. N. Rylander, *J. Org. Chem.* **1959**, *24*, 708. c) D. Evans, J. A. Osborn, F. H. Jardine, G. Wilkinson, *Nature* **1965**, *208*, 1203.

[2] B. M. Trost, M. U. Frederiksen, M. T. Rudd, *Angew. Chem. Int. Ed.* **2005**, *44*, 6630.
[3] S. Miao, Z. Liu, B. Han, J. Huang, Z. Sun, J. Zhang, T. Jiang, *Angew. Chem. Int. Ed.* **2006**, *45*, 266.
[4] Z. Sun, Z. Liu, B. Han, Y. Wang, J. Du, Z. Xie, G. Han, *Adv. Mater.* **2005**, *17*, 928.
[5] W. Zhou, J. M. Thomas, D. S. Shephard, B. F. G. Johnson, D. Ozkaya, T. Maschmeyer, R. G. Bell, Q. Ge, *Science* **1998**, *280*, 705.
[6] M. L. Kantam, B. P. C. Rao, B. M. Choudary, B. Sreedhara, *Adv. Synth. Catal.* **2006**, *348*, 1970.
[7] K. van Gorp, E. Boerman, C. V. Cavenaghi, P. H. Berben, *Catal. Today* **1999**, *52*, 349.
[8] B. Kusserow, S. Schimpf, P. Claus, *Adv. Synth. Catal.* **2003**, *345*, 289.
[9] a) R. Ryoo, S. H. Joo, M. Kruk, M. Jaroniec, *Adv. Mater.* **2001**, *13*, 677. b) A. Stein, *Adv. Mater.* **2003**, *15*, 763. c) A.-H. Lu, F. Schüth, *Adv. Mater.* **2006**, *18*, 1793. d) J. Lee, J. Kim, T. Hyeon, *Adv. Mater.* **2006**, *18*, 2073. e) F. Su, Z. Zhou, J. Liu, X. N. Tian, X. S. Zhao, in *Chemistry and Physics of Carbon*, Vol. 30 (Ed: L. R. Radovic), Marcel Dekker, New York, **2007**, in press.
[10] a) S. H. Joo, S. J. Choi, I. Oh, J. Kwak, Z. Liu, O. Terasaki, R. Ryoo, *Nature* **2001**, *412*, 169. b) W. S. Ahn, K. I. Min, Y. M. Chung, H. K. Rhee, S. H. Joo, R. Ryoo, *Stud. Surf. Sci. Catal.* **2001**, *135*, 313. c) A.-H. Lu, W. Schmidt, N. Matoussevitch, H. Bönnemann, B. Spliethoff, B. Tesche, E. Bill, W. Kiefer, F. Schüth, *Angew. Chem. Int. Ed.* **2004**, *43*, 4303. d) G. S. Chai, I. S. Shin, J. S. Yu, *Adv. Mater.* **2004**, *16*, 2057. e) W. C. Choi, S. I. Woo, M. K. Jeon, J. M. Sohn, M. R. Kim, H. J. Jeon, *Adv. Mater.* **2005**, *17*, 446. f) F. Su, X. S. Zhao, Y. Wang, J. Zeng, Z. Zhou, J. Y. Lee, *J. Phys. Chem. B* **2005**, *109*, 20200. g) D. Lee, J. Lee, J. Kim, J. Kim, H. B. Na, B. Kim, C.-H. Shin, J. H. Kwak, A. Dohnalkova, J. W. Grate, T. Hyeon, H.-S. Kim, *Adv. Mater.* **2005**, *17*, 2828. h) S.-H. Liu, R.-F. Lu, S.-J. Huang, A.-Y. Lo, S.-H. Chien, S.-B. Liu, *Chem. Commun.* **2006**, 3435.
[11] a) S. M. Holmes, P. Foran, E. P. L. Robertsa, J. M. Newton, *Chem. Commun.* **2005**, 1912. b) J. Lee, S. Jin, Y. Hwang, J.-G. Park, H. M. Park, T. Hyeon, *Carbon* **2005**, *43*, 2536. c) I.-S. Park, M. Choi, T.-W. Kim, R. Ryoo, *J. Mater. Chem.* **2006**, *16*, 3409. d) D. Nguyen-Thanh, T. J. Bandosz, *Microporous Mesoporous Mater.* **2006**, *92*, 47.
[12] J. Lee, D. Lee, E. Oh, J. Kim, Y.-P. Kim, S. Jin, H.-S. Kim, Y. Hwang, J. H. Kwak, J.-G. Park, C.-H. Shin, J. Kim, T. Hyeon, *Angew. Chem. Int. Ed.* **2005**, *44*, 7427.
[13] a) S. Ikeda, S. Ishino, T. Harada, N. Okamoto, T. Sakata, H. Mori, S. Kuwabata, T. Torimoto, M. Matsumura, *Angew. Chem. Int. Ed.* **2006**, *45*, 7063. b) Y. H. Ng, S. Ikeda, T. Harada, S. Higashida, T. Sakata, H. Mori, M. Matsumura, *Adv. Mater.* **2007**, *19*, 597.
[14] a) F. Su, J. Zeng, X. Bao, Y. Yu, J. Y. Lee, X. S. Zhao, *Chem. Mater.* **2005**, *17*, 3960. b) F. Su, J. Zeng, Y. Yu, L. Lv, J. Y. Lee, X. S. Zhao, *Carbon* **2005**, *43*, 2366.
[15] A. Roucoux, J. Schulz, H. Patin, *Chem. Rev.* **2002**, *102*, 3757.
[16] a) A. Stanislaus, B. H. Cooper, *Catal. Rev. – Sci. Eng.* **1994**, *36*, 75. b) B. H. Cooper, B. B. L. Donnis, *Appl. Catal. A* **1996**, *137*, 203.
[17] T. W. Hansen, J. B. Wagner, P. L. Hansen, S. Dahl, H. Topsøe, C. J. H. Jacobsen, *Science* **2001**, *294*, 1508.
[18] a) Y. Tian, Z. Hu, Y. Yang, X. Wang, X. Chen, H. Xu, Q. Wu, W. Ji, Y. Chen, *J. Am. Chem. Soc.* **2004**, *126*, 1180. b) K. Villani, C. E. A. Kirschhock, D. Liang, G. Van Tendeloo, J. A. Martens, *Angew. Chem. Int. Ed.* **2006**, *45*, 3106.
[19] P. G. J. Koopman, A. P. G. Kieboom, H. van Bekkum, J. W. E. Coenen, *Carbon* **1979**, *17*, 399.
[20] P. Barbaro, C. Bianchini, V. Dal Santo, A. Meli, S. Moneti, R. Psaro, A. Scaffidi, L. Sordelli, F. Vizza, *J. Am. Chem. Soc.* **2006**, *128*, 7065.
[21] W. C. Conner, Jr., J. L. Falconer, *Chem. Rev.* **1995**, *95*, 759.
[22] *Spillover and Migration of Surface Species on Catalysts*, *Studies in Surface Science and Catalysis 112* (Eds: C. Li, Q. Xin), Elsevier Science, The Netherlands, **1997**.
[23] U. Roland, T. Braunschweig, F. Roessner, *J. Mol. Catal. A: Chem.* **1997**, *127*, 61.
[24] E. Keren, A. Soffer, *J. Catal.* **1977**, *50*, 43.
[25] a) M. Boudart, A. W. Aldag, M. A. Vannice, *J. Catal.* **1970**, *18*, 46. b) R. B. Levy, M. Boudart, *J. Catal.* **1974**, *32*, 304. c) S. T. Srinivas, P. K. Rao, *J. Catal.* **1994**, *148*, 470. d) A. Lueking, R. T. Yang, *AIChE J.* **2003**, *49*, 1556. e) A. J. Lachawiec, Jr., G. Qi, R. T. Yang, *Langmuir* **2005**, *21*, 11418.
[26] a) T. S. King, X. Wu, B. C. Gerstein, *J. Am. Chem. Soc.* **1986**, *108*, 6056. b) P. Badenes, L. Daza, I. Rodriguez-Ramos, A. Guerrero-Ruiz, *Stud. Surf. Sci. Catal.* **1997**, *112*, 241. c) H. Ishikawa, J. N. Kondo, K. Domen, *J. Phys. Chem. B* **1999**, *103*, 3229.
[27] a) S. D. Lin, M. A. Vannice, *J. Catal.* **1993**, *143*, 539. b) T. Ioannides, X. E. Verykios, *J. Catal.* **1993**, *143*, 175.
[28] M. Cerro-Alarcón, A. Maroto-Valiente, I. Rodríguez-Ramos, A. Guerrero-Ruiz, *Carbon* **2005**, *43*, 2711.
[29] C. Liang, Z. Wei, Q. Xin, C. Li, *Appl. Catal., A* **2001**, *208*, 193.
[30] P. Kluson, L. Cerveny, *Appl. Catal. A.* **1995**, *128*, 13.
[31] Y. Li, R. T. Yang, *J. Am. Chem. Soc.* **2006**, *128*, 8136.
[32] a) D. R. Rolison, P. L. Hagans, K. E. Swider, J. W. Long, *Langmuir* **1999**, *15*, 774. b) S. Zhu, H. Zhou, D. Yan, *Microporous Mesoporous Mater.* **2007**, *100*, 227.
[33] D. Zhao, J. Feng, Q. Huo, N. Melosh, G. H. Fredrickson, B. F. Chmelka, G. D. Stucky, *Science* **1998**, *279*, 548.
[34] a) P. Gallezot, N. Nicolaus, G. Flèche, P. Fuertes, A. Perrard, *J. Catal.* **1998**, *180*, 51. b) L. Fabre, P. Gallezot, A. Perrard, *J. Catal.* **2002**, *208*, 247.